arXiv:1202.3588v1 [math.AP] 16 Feb 2012

INTERFACES SUPPORTING SURFACE GAP SOLITON GROUND STATES IN THE 1D NONLINEAR SCHRÖDINGER EQUATION

TOMÁŠ DOHNAL, KAORI NAGATOU, MICHAEL PLUM, AND WOLFGANG REICHEL

ABSTRACT. We consider the problem of verifying the existence of H^1 ground states of the 1D nonlinear Schrödinger equation for an interface of two periodic structures:

$$-u'' + V(x)u - \lambda u = \Gamma(x)|u|^{p-1}u \quad \text{on } \mathbb{R}$$

with $V(x) = V_1(x), \Gamma(x) = \Gamma_1(x)$ for $x \geq 0$ and $V(x) = V_2(x), \Gamma(x) = \Gamma_2(x)$ for $x < 0$. Here $V_1, V_2, \Gamma_1, \Gamma_2$ are periodic, $\lambda < \min \sigma(-\frac{d^2}{dx^2} + V)$, and $p > 1$. The article [T. Dohnal, M. Plum and W. Reichel, "Surface Gap Soliton Ground States for the Nonlinear Schrödinger Equation," *Comm. Math. Phys.* **308**, 511-542 (2011)] provides in the 1D case an existence criterion in the form of an integral inequality involving the linear potentials V_1, V_2 and the Bloch waves of the operators $-\frac{d^2}{dx^2} + V_{1,2} - \lambda$. We choose here the classes of piecewise constant and piecewise linear potentials $V_{1,2}$ and check this criterion for a set of parameter values. In the piecewise constant case the Bloch waves are calculated explicitly and in the piecewise linear case verified enclosures of the Bloch waves are computed numerically. The integrals in the criterion are evaluated via interval arithmetic so that rigorous existence statements are produced. Examples of interfaces supporting ground states are reported including such, for which ground state existence follows for all periodic $\Gamma_{1,2}$ with $\operatorname{ess\,sup} \Gamma_{1,2} > 0$.

1. INTRODUCTION

An interface between two nonlinear periodic media in the $n-$dimensional nonlinear Schrödinger model can act as a waveguide so that localized solutions, so called surface gap solitons (SGS), exist as shown analytically in [3]. Experimentally such waveguiding has been demonstrated in nonlinear photonic crystals, see e.g. [9,11,12]. There are also a number of numerical observations of SGSs in the 1D and 2D nonlinear Schrödinger equation (NLS), see e.g. [1,2,5,6].

In [3] an existence criterion for strong ground states of the $n-$dimensional NLS

$$(n\text{-NLS}) \qquad (-\Delta + V(x) - \lambda)u = \Gamma(x)|u|^{p-1}u, \ x \in \mathbb{R}^n$$

was proved with $V(x) = V_1(x), \Gamma(x) = \Gamma_1(x)$ for $x_1 \geq 0$ and $V(x) = V_2(x), \Gamma(x) = \Gamma_2(x)$ for $x_1 < 0$ under the condition $\lambda < \min \sigma(-\Delta + V)$. The functions $V_1, V_2, \Gamma_1, \Gamma_2$ are assumed periodic in each coordinate direction and the exponent p satisfies $p \in (1, 2^*)$, where $2^* = \frac{2n}{n-2}$ if $n \geq 3$ and $2^* = \infty$ if $n = 1, 2$. A strong ground state is defined to be a minimizer of the corresponding total energy $\int_{\mathbb{R}^n} \frac{1}{2}(|\nabla u|^2 + V(x)u^2) - \frac{1}{p+1}|u|^{p+1} dx$ restricted to the Nehari manifold $N = \{u \in H^1(\mathbb{R}^n) \setminus \{0\} : \int_{\mathbb{R}^n} |\nabla u|^2 + (V(x) - \lambda)u^2 - \Gamma(x)|u|^{p+1} dx = 0\}$. The

---

Date: February 17, 2012.

2000 *Mathematics Subject Classification.* Primary: 35Q55, 78M30, 65G20; Secondary: 35J20, 35Q60.

Key words and phrases. nonlinear Schrödinger equation, surface gap soliton, ground state, variational methods, interface, periodic material, verified numerical enclosures.

results of [3] include sufficient conditions for the existence of strong ground states. These conditions involve information about the strong ground states[1] w_1, w_2 of the purely periodic problems (n-NLS) with $V = V_1, \Gamma = \Gamma_1$ on $\mathbb{R}^n$ and $V = V_2, \Gamma = \Gamma_2$ on $\mathbb{R}^n$ respectively. In the case $n = 1$ these conditions could be formulated in terms of the Bloch waves of the two purely periodic linear problems. As neither the ground states w_1, w_2 nor the Bloch waves are generally known explicitly, [3] did not produce explicit examples of ground state supporting interfaces except for an example where the potentials are related by scaling: $V_1(x) = k^2 V_2(kx)$, $\Gamma_1(x) = \gamma^2 \Gamma_2(kx)$ with certain conditions on k and γ, see Theorem 5 in [3]. All other existence examples were asymptotic; either in λ or in $\Gamma_1 - \Gamma_2$.

The most practical existence criteria in [3] are those for the 1D case $n = 1$. In this article we provide a number of explicit 1D examples of interfaces satisfying these criteria. We consider, therefore

$$-u'' + V(x)u - \lambda u = \Gamma(x)|u|^{p-1}u \text{ on } \mathbb{R} \tag{1.1}$$

with

$$V(x) = \begin{cases} V_1(x), & x \geq 0, \\ V_2(x), & x < 0, \end{cases} \tag{1.2}$$

and

$$\Gamma(x) = \begin{cases} \Gamma_1(x), & x \geq 0, \\ \Gamma_2(x), & x < 0 \end{cases} \tag{1.3}$$

under the assumptions

- (H1) $V_1, V_2, \Gamma_1, \Gamma_2$ are 1-periodic,
- (H2) $\operatorname{ess\,sup} \Gamma_i > 0$, $i = 1, 2$,
- (H3) $1 < p < \infty$,
- (H4) $\lambda < \min \sigma(-\frac{d^2}{dx^2} + V)$,

which were needed in [3].

Next, recall the criterion given in Theorem 7 in [3] for the existence of SGS ground states of (1.1).

Theorem 1. *Assume (H1)–(H4) and for* $i = 1, 2$ *define by* c_i *the energy of a strong ground state of* $(-\frac{d^2}{dx^2} + V_i(x) - \lambda)u = \Gamma_i(x)|u|^{p-1}u$ *on* $\mathbb{R}$.

(a) *If* $c_1 \leq c_2$, *then a sufficient condition for the existence of a strong ground state of* (1.1) *is*

$$I_1 := \int_{-1}^{0} \Big(V_2(x) - V_1(x)\Big) u_-^{(1)}(x)^2 \, dx < 0, \tag{1.4}$$

where $u_-^{(1)}(x) = p_-^{(1)}(x) e^{\kappa_1 x}$, *with* $\kappa_1 > 0$ *and* $p_-^{(1)}$ *periodic, is the Bloch mode decaying at* $-\infty$ *of* $-\frac{d^2}{dx^2} + V_1(x) - \lambda$.

---

[1] The existence of strong ground states of the purely periodic problem on $\mathbb{R}^n$ was proved in [8].

(b) *If* $c_1 \geq c_2$*, then a sufficient condition for the existence of a strong ground state of* (1.1) *is*

$$I_2 := \int_0^1 \Big(V_1(x) - V_2(x)\Big) u_+^{(2)}(x)^2 \, dx < 0, \tag{1.5}$$

where $u_+^{(2)}(x) = p_+^{(2)}(x) e^{-\kappa_2 x}$*, with* $\kappa_2 > 0$ *and* $p_+^{(2)}$ *periodic, is the Bloch mode decaying at* $+\infty$ *of* $-\frac{d^2}{dx^2} + V_2(x) - \lambda$.

When the ordering of c_1, c_2 is unknown, Theorem 1 can still be used by establishing negativity of *both* of the integrals I_1 and I_2:

Corollary 2. *If both* $I_1, I_2 < 0$*, then a strong ground state exists irrespectively of the order of* c_1 *and* c_2*, and thus, of the choice of* Γ_1, Γ_2 *and* p *(within the assumptions (H1)-(H3)).*

As seen from (1.4) and (1.5), any ordering $V_1(x) \geq V_2(x)$ or $V_1(x) \leq V_2(x)$ on $[0,1]$ leads to $I_1 \leq 0 \leq I_2$ or $I_2 \leq 0 \leq I_1$, whence the assumption of corollary 2 is not satisfied.

If information on the ordering of the ground state energies c_1, c_2 is available, the corresponding criterion (a) or (b) in Theorem 1 can be checked. This is the case, for instance, with the dislocation interface

$$V(x) = \begin{cases} V_0(x + \tau_1), & x \geq 0, \\ V_0(x - \tau_2), & x < 0, \end{cases} \qquad \Gamma(x) = \begin{cases} \Gamma_0(x + \tau_1), & x \geq 0, \\ \Gamma_0(x - \tau_2), & x < 0, \end{cases} \tag{1.6}$$

where V_0, Γ_0 are $1-$periodic, $\operatorname{ess\,sup} \Gamma_0 > 0$, and where $\tau_1, \tau_2 \in [0, d]$ are the dislocation parameters. In this case $c_1 = c_2$ so that we have

Corollary 3. *For the interface* (1.6) *suppose* $I_1 < 0$ *or* $I_2 < 0$*. Then there exists a strong ground state irrespectively of the choice of* p *(within (H3)) and of* Γ_0 *(within the above assumptions).*

We will use direct constructive approaches to verify the respective conditions (1.4) and (1.5). These require mainly the Bloch waves of the two purely periodic linear problems on $\mathbb{R}$. We consider two types of potentials $V_{1,2}$: piecewise constant and piecewise linear. For piecewise constant potentials we calculate the needed Bloch modes in closed form by hand, so that we can check these conditions directly. For piecewise linear potentials we use a computer-assisted approach, i.e. we compute verified enclosures for the Bloch modes, and use these to enclose the integrals I_1 and I_2 in (1.4) and (1.5). These computer-assisted results are completely verified and thus give a rigorous mathematical proof since all numerical errors are taken into account. In principle, even much more general potentials can be treated by this approach; we have chosen piecewise linear ones for simplicity.

In the rest of the paper we impose the condition

$$\lambda < \min\{\inf V_1, \inf V_2\},$$

which ensures (H4) without having to actually calculate the spectrum.

In Section 2 below we consider interfaces with piecewise constant potentials V_1 and V_2 and in Section 3 we study the case of piecewise linear potentials.

2. PIECEWISE CONSTANT POTENTIALS V_1 AND V_2

When the potentials V_1 and V_2 are piecewise constant, the integrals I_1, I_2 can be calculated explicitly although the closed form involves the inverse of a transcendental function. We calculate the formulas for I_1, I_2 explicitly and evaluate these numerically for a set of parameter values. The evaluation is done in interval arithmetic (using the Matlab toolbox Intlab [10]). The resulting values of I_1, I_2 are thus enclosed in intervals and when the supremum of such an interval is negative, the corresponding integral I_1 or I_2 is then verified to be negative.

2.1. **Bloch Waves for a Piecewise Constant Potential.**

Let

$$V_0(x) = \begin{cases} a, & 0 \le x < s, \\ b, & s \le x < 1 \end{cases} \tag{2.1}$$

with $a, b \in \mathbb{R}$ and $s \in (0,1)$.

The Bloch waves of $-u'' + V_0(x)u = \lambda u$ on $\mathbb{R}$ have the form

$$u_\pm(x) = p_\pm(x) e^{\mp\kappa x} \quad \text{with } p_\pm(x+1) = p_\pm(x), \kappa > 0$$

since λ lies in the resolvent set of $-\frac{d^2}{dx^2} + V_0$, see [4]. At the same time, due to the piecewise constant nature of V_0

$$u_\pm(x) = \begin{cases} \xi_1^\pm e^{x\sqrt{a-\lambda}} + \xi_2^\pm e^{-x\sqrt{a-\lambda}}, & 0 \le x < s, \\ \xi_3^\pm e^{x\sqrt{b-\lambda}} + \xi_4^\pm e^{-x\sqrt{b-\lambda}}, & s \le x < 1. \end{cases} \tag{2.2}$$

The vectors $\xi^\pm$ are determined via the C^1 condition for $u_\pm(x)$ at $x = s$ and the condition that the Floquet multipliers of $u_\pm$ are $e^{\mp\kappa}$ respectively. For ξ^+ we thus obtain the system

$$A(\kappa)\xi^+ = 0, \qquad A(\kappa) = \begin{pmatrix} e^{s\sqrt{a-\lambda}} & e^{-s\sqrt{a-\lambda}} & -e^{s\sqrt{b-\lambda}} & -e^{-s\sqrt{b-\lambda}} \\ \sqrt{a-\lambda}\, e^{s\sqrt{a-\lambda}} & -\sqrt{a-\lambda}\, e^{-s\sqrt{a-\lambda}} & -\sqrt{b-\lambda}\, e^{s\sqrt{b-\lambda}} & \sqrt{b-\lambda}\, e^{-s\sqrt{b-\lambda}} \\ -e^{-\kappa} & -e^{-\kappa} & e^{\sqrt{b-\lambda}} & e^{-\sqrt{b-\lambda}} \\ -\sqrt{a-\lambda}\, e^{-\kappa} & \sqrt{a-\lambda}\, e^{-\kappa} & \sqrt{b-\lambda}\, e^{\sqrt{b-\lambda}} & -\sqrt{b-\lambda}\, e^{-\sqrt{b-\lambda}} \end{pmatrix}.$$

Solving $\det(A(\kappa)) = 0$ yields

$$\begin{aligned} \cosh(\kappa) = \frac{1}{4\sqrt{a-\lambda}\sqrt{b-\lambda}} \Big[& (\sqrt{a-\lambda} + \sqrt{b-\lambda})^2 \cosh\left(s\sqrt{a-\lambda} + (1-s)\sqrt{b-\lambda}\right) \\ & -(\sqrt{a-\lambda} - \sqrt{b-\lambda})^2 \cosh\left(s\sqrt{a-\lambda} - (1-s)\sqrt{b-\lambda}\right) \Big]. \end{aligned} \tag{2.3}$$

The solution vector ξ^+ is proportional to

$$\begin{aligned}
\xi_1^+ &= \frac{e^{-s\sqrt{a-\lambda}}}{2\left(e^{s(\sqrt{a-\lambda}+\sqrt{b-\lambda})-\kappa} - e^{\sqrt{b-\lambda}}\right)} \Big[4e^{s\sqrt{a-\lambda}-\kappa}\sqrt{a-\lambda}\sqrt{b-\lambda} \\
&\quad - \left(\sqrt{a-\lambda}+\sqrt{b-\lambda}\right)^2 e^{(s-1)\sqrt{b-\lambda}} + \left(\sqrt{a-\lambda}-\sqrt{b-\lambda}\right)^2 e^{(1-s)\sqrt{b-\lambda}}\Big], \\
\xi_2^+ &= (a-b)\frac{\sinh((1-s)\sqrt{b-\lambda})}{e^{s\sqrt{b-\lambda}-\kappa} - e^{\sqrt{b-\lambda}-s\sqrt{a-\lambda}}}, \\
\xi_3^+ &= \left(a-\lambda+\sqrt{a-\lambda}\sqrt{b-\lambda}\right)\frac{e^{(\sqrt{a-\lambda}-\sqrt{b-\lambda})s-\kappa} - e^{-\sqrt{b-\lambda}}}{e^{(\sqrt{a-\lambda}+\sqrt{b-\lambda})s-\kappa} - e^{\sqrt{b-\lambda}}}, \\
\xi_4^+ &= \lambda - a + \sqrt{a-\lambda}\sqrt{b-\lambda}.
\end{aligned} \tag{2.4}$$

The system for ξ^- reads $A(-\kappa)\xi^- = 0$, so that

$$\xi^-(\kappa) = \xi^+(-\kappa). \tag{2.5}$$

2.2. **Dislocation Interface.**

Let us consider the dislocation interface (1.6) with $\tau_1 = \tau_2 =: \tau$ for the piecewise constant potential

$$V_0(x) = \begin{cases} a, & 0 \le x < 1/2, \\ b, & 1/2 \le x < 1 \end{cases}$$

with $a, b \in \mathbb{R}$. In this case $u_\pm^{(1)}(x) = u_\pm(x+\tau)$ and $u_\pm^{(2)}(x) = u_\pm(x-\tau)$ with $u_\pm$ in (2.2), $\xi^\pm$ in (2.4), (2.5) and κ in (2.3), where we set $s = 1/2$.

A direct integration then produces for $0 < \tau < 1/2$

$$\begin{aligned}
I_1(\tau) &= \frac{b-a}{2\sqrt{a-\lambda}} e^{-2\kappa} \Big[\xi_1^{-2} e^{(1+2\tau)\sqrt{a-\lambda}} \left(e^{(2\tau-1)\sqrt{a-\lambda}} - 1\right)\left(1 - e^{-2\tau\sqrt{a-\lambda}}\right) \\
&\qquad + \xi_2^{-2} e^{-(1+2\tau)\sqrt{a-\lambda}} \left(e^{(1-2\tau)\sqrt{a-\lambda}} - 1\right)\left(e^{2\tau\sqrt{a-\lambda}} - 1\right)\Big] \\
&\quad + \frac{b-a}{2\sqrt{b-\lambda}} e^{-2\kappa} \Big[\xi_3^{-2} e^{(1+2\tau)\sqrt{b-\lambda}} \left(e^{(1-2\tau)\sqrt{b-\lambda}} - 1\right)\left(e^{2\tau\sqrt{b-\lambda}} - 1\right) \\
&\qquad + \xi_4^{-2} e^{-(1+2\tau)\sqrt{b-\lambda}} \left(e^{(2\tau-1)\sqrt{b-\lambda}} - 1\right)\left(1 - e^{-2\tau\sqrt{b-\lambda}}\right)\Big],
\end{aligned} \tag{2.6}$$

and for $1/2 \le \tau < 1$

$$\begin{aligned}
I_1(\tau) &= \frac{b-a}{2\sqrt{a-\lambda}} e^{-2\kappa} \Big[\xi_1^{-2} e^{(1+2\tau)\sqrt{a-\lambda}} \left(e^{(1-2\tau)\sqrt{a-\lambda}} - 1\right)\left(e^{2(\tau-1)\sqrt{a-\lambda}} - 1\right) \\
&\qquad + \xi_2^{-2} e^{-(1+2\tau)\sqrt{a-\lambda}} \left(e^{(2\tau-1)\sqrt{a-\lambda}} - 1\right)\left(1 - e^{2(1-\tau)\sqrt{a-\lambda}}\right)\Big] \\
&\quad + \frac{b-a}{2\sqrt{b-\lambda}} e^{-2\kappa} \Big[\xi_3^{-2} e^{2(\tau+1)\sqrt{b-\lambda}} \left(e^{(1-2\tau)\sqrt{b-\lambda}} - 1\right)\left(1 - e^{2(\tau-1)\sqrt{b-\lambda}}\right) \\
&\qquad + \xi_4^{-2} e^{-2(\tau+1)\sqrt{b-\lambda}} \left(e^{(2\tau-1)\sqrt{b-\lambda}} - 1\right)\left(e^{2(1-\tau)\sqrt{b-\lambda}} - 1\right)\Big].
\end{aligned} \tag{2.7}$$

For the integral I_2 we have for $0 < \tau < 1/2$

$$
\begin{aligned}
I_2(\tau) = \frac{a-b}{2\sqrt{a-\lambda}} &\Big[{\xi_1^+}^2 e^{(1-2\tau)\sqrt{a-\lambda}} \left(e^{(2\tau-1)\sqrt{a-\lambda}} - 1\right)\left(1 - e^{-2\tau\sqrt{a-\lambda}}\right) \\
&\quad + {\xi_2^+}^2 e^{(2\tau-1)\sqrt{a-\lambda}} \left(e^{(1-2\tau)\sqrt{a-\lambda}} - 1\right)\left(e^{2\tau\sqrt{a-\lambda}} - 1\right)\Big] \\
+ \frac{a-b}{2\sqrt{b-\lambda}} &\Big[{\xi_3^+}^2 e^{(1-2\tau)\sqrt{b-\lambda}} \left(e^{(1-2\tau)\sqrt{b-\lambda}} - 1\right)\left(e^{2\tau\sqrt{b-\lambda}} - 1\right) \\
&\quad + {\xi_4^+}^2 e^{(2\tau-1)\sqrt{b-\lambda}} \left(e^{(2\tau-1)\sqrt{b-\lambda}} - 1\right)\left(1 - e^{-2\tau\sqrt{b-\lambda}}\right)\Big],
\end{aligned}
\tag{2.8}
$$

and for $1/2 \le \tau < 1$

$$
\begin{aligned}
I_2(\tau) = \frac{a-b}{2\sqrt{a-\lambda}} &\Big[{\xi_1^+}^2 e^{(1-2\tau)\sqrt{a-\lambda}} \left(e^{(1-2\tau)\sqrt{a-\lambda}} - 1\right)\left(e^{2(\tau-1)\sqrt{a-\lambda}} - 1\right) \\
&\quad + {\xi_2^+}^2 e^{(2\tau-1)\sqrt{a-\lambda}} \left(e^{(2\tau-1)\sqrt{a-\lambda}} - 1\right)\left(1 - e^{2(1-\tau)\sqrt{a-\lambda}}\right)\Big] \\
+ \frac{a-b}{2\sqrt{b-\lambda}} &\Big[{\xi_3^+}^2 e^{2(1-\tau)\sqrt{b-\lambda}} \left(e^{(1-2\tau)\sqrt{b-\lambda}} - 1\right)\left(1 - e^{2(\tau-1)\sqrt{b-\lambda}}\right) \\
&\quad + {\xi_4^+}^2 e^{2(\tau-1)\sqrt{b-\lambda}} \left(e^{(2\tau-1)\sqrt{b-\lambda}} - 1\right)\left(e^{2(1-\tau)\sqrt{b-\lambda}} - 1\right)\Big].
\end{aligned}
\tag{2.9}
$$

For the dislocation interfaces with $a = 1$ and $b \in \{2, 6\}$ Fig. 1 shows regions of the (τ, λ) plane where the integral I_1 or I_2 is negative, i.e. where ground state existence is guaranteed. These regions were computed using interval arithmetic. The domain $[0, 1] \times [-2, 0.98]$ in the (τ, λ)-plane was completely covered[2] by two dimensional intervals (squares) of size 1/600 along each dimension and when for a given square the interval arithmetic evaluation produced $I_k < 0$ (which means a negative supremum of the enclosure of I_k), the square was shaded. Note that it is a priori clear that both I_1 and I_2 are zero at $\tau = 0, 1/2$, and 1 because for these values $V_0(x + \tau) - V_0(x - \tau) \equiv 0$ due to the 1−periodicity of V_0 and the integrands in I_1, I_2 thus vanish . The use of interval arithmetic in the computations then necessarily results in small neighborhoods of $\tau = 0, 1/2, 1$ where the sign of the integrals cannot be determined.

As Fig. 1 shows, ground state existence is guaranteed in both cases $b = 2$ and $b = 6$ in almost the entire parameter domain $(\tau, \lambda) \in [0, 1] \times [-2, 0.98]$. Interestingly, in both cases we find regions where I_1 *and* I_2 are negative. In these regions ground state existence thus follows by Corollary 2 irrespectively of the nonlinear coefficients Γ_1 and Γ_2 and of the order p because both criteria in Theorem 1 are satisfied. The coefficients and the order can be freely changed (within (H1)-(H3)) and the ground state will still exist! In particular, Γ_1, Γ_2 do not have to be related by the dislocation property in (1.6).

In Fig. 2 and 3 the enclosures of $\sqrt{a-\lambda}\sqrt{b-\lambda}\, I_1$ and $\sqrt{a-\lambda}\sqrt{b-\lambda}\, I_2$ as functions of τ are plotted for the two examples in Fig. 1 at two values of λ. The quantities I_1, I_2 contain $\sqrt{a-\lambda}$ and $\sqrt{b-\lambda}$ in the denominator. To reduce the amount of round off error for λ close to $\min\{a, b\}$, we plot $\sqrt{a-\lambda}\sqrt{b-\lambda}\, I_{1,2}$. Note that in Fig. 2 (b) the τ-region, where both

---

[2] All intervals whose endpoints are not floating-point numbers are safely enclosed in slightly larger intervals by use of Intlab.

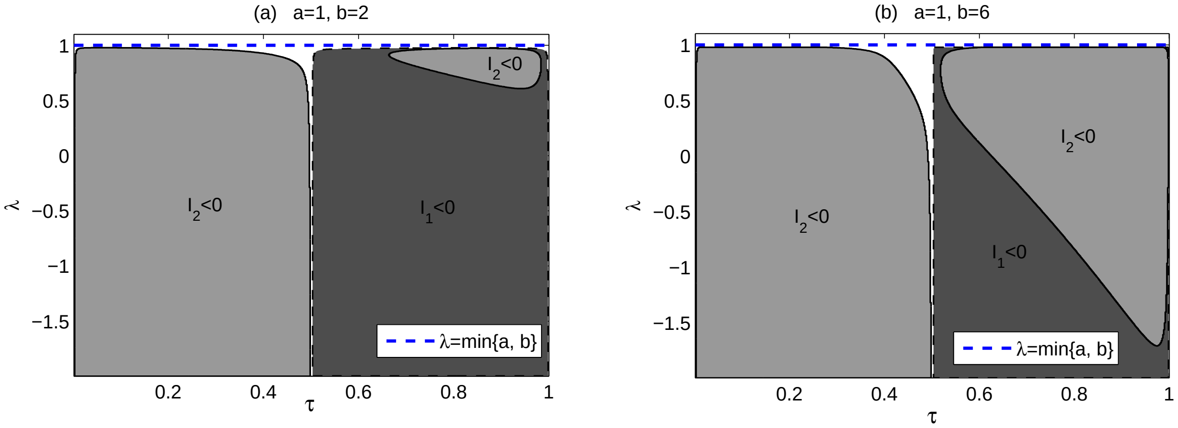

FIGURE 1. Regions in the (τ, λ) plane, where suprema of the enclosures of I_1 and I_2 are negative for the dislocation interface with a piecewise constant V_0 and $a = 1$. (a) $b = 2$; (b) $b = 6$ (computations performed in interval arithmetic).

I_1 and I_2 are negative, is larger than at the corresponding value of λ in Fig. 1 (a). This is because Fig. 1 is produced using two dimensional intervals (intervals in the (τ, λ)-plane) for input while in Fig. 2 the input are one dimensional intervals. The larger overestimation due to interval arithmetic in the case of two dimensional intervals leads to a smaller region where negativity of I_1 and I_2 is verified.

In Fig. 3 (b) a small left neighborhood of $\tau = 1/2$ is visible where the infima of the enclosures of both I_1 and I_2 are positive so that existence of strong ground states cannot be concluded based on Theorem 1.

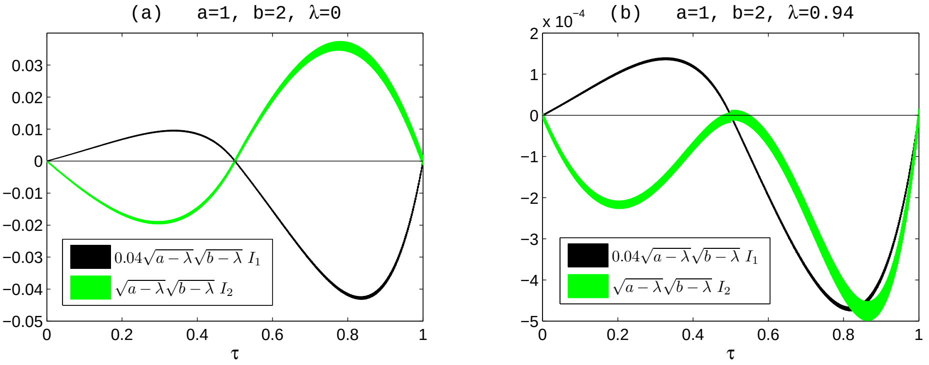

FIGURE 2. Scaled plots of the interval enclosures of $\sqrt{a-\lambda}\sqrt{b-\lambda}\ I_1$ and $\sqrt{a-\lambda}\sqrt{b-\lambda}\ I_2$ as functions of τ corresponding to Fig. 1 (a). In (a) $\lambda = 0$ and in (b) $\lambda = 0.94$ (computations performed in interval arithmetic with the τ-interval width 1/600).

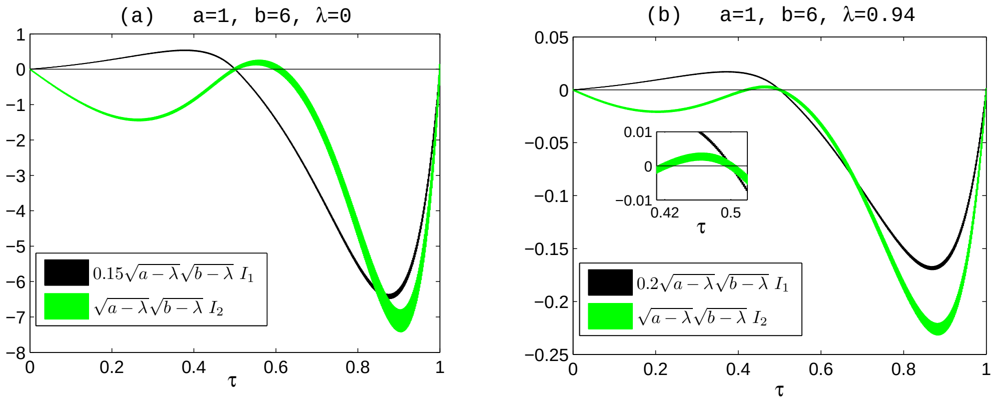

FIGURE 3. Scaled plots of the interval enclosures of $\sqrt{a-\lambda}\sqrt{b-\lambda}\ I_1$ and $\sqrt{a-\lambda}\sqrt{b-\lambda}\ I_2$ as functions of τ with a and b as in Fig. 1 (b). In (a) $\lambda = 0$ and in (b) $\lambda = 0.94$ (computations performed in interval arithmetic with the τ-interval width 1/600).

2.3. **Interface with no Knowledge about c_1, c_2.**

Here we consider a general interface (1.2), (1.3) with the piecewise constant structure (2.1) for both V_1 and V_2. In detail, V_1 is given by (2.1) with (a, b, s) replaced by (a_1, b_1, s_1) and V_2 is given by (2.1) with (a, b, s) replaced by (a_2, b_2, s_2). For simplicity we choose the jump locations in the middle of the periodicity cell: $s_1 = s_2 = 1/2$.

The Bloch waves $u_\pm^{(1)}$ are now given by (2.2) and (2.3)-(2.5) with (a, b, s) replaced by $(a_1, b_1, 1/2)$. We denote the resulting κ in (2.3) by κ_1. Analogously we obtain $u_\pm^{(2)}$ and denote the resulting vectors in (2.4),(2.5) by $\zeta^\pm$.

Because the ordering of c_1 and c_2 is unknown in this case, Theorem 1 can be used to prove ground state existence only if both I_1 and I_2 are negative. If this occurs, the existence of a strong ground state is then completely independent of the nonlinear periodic coefficients Γ_1, Γ_2 and of p (within (H1)-(H3)). We show below that similarly to the dislocation example such cases can be found here as well.

The integrals from Theorem 1 now become

(2.10)

$$\begin{aligned} I_1 = {} & e^{-2\kappa_1}(a_2-a_1)\xi_1^-\xi_2^- + \frac{e^{-2\kappa_1}(a_2-a_1)}{2\sqrt{a_1-\lambda}}\left[{\xi_1^-}^2\left(e^{\sqrt{a_1-\lambda}}-1\right)+{\xi_2^-}^2\left(1-e^{-\sqrt{a_1-\lambda}}\right)\right] \\ & + e^{-2\kappa_1}(b_2-b_1)\xi_3^-\xi_4^- + \frac{e^{-2\kappa_1}(b_2-b_1)}{2\sqrt{b_1-\lambda}}\left[{\xi_3^-}^2\left(e^{2\sqrt{b_1-\lambda}}-e^{\sqrt{b_1-\lambda}}\right)+{\xi_4^-}^2\left(e^{-\sqrt{b_1-\lambda}}-e^{-2\sqrt{b_1-\lambda}}\right)\right], \end{aligned}$$

and

$$
\begin{aligned}
I_2 &= (a_1 - a_2)\zeta_1^+\zeta_2^+ + \frac{a_1 - a_2}{2\sqrt{a_2 - \lambda}}\left[{\zeta_1^+}^2\left(e^{\sqrt{a_2-\lambda}} - 1\right) + {\zeta_2^+}^2\left(1 - e^{-\sqrt{a_2-\lambda}}\right)\right] \\
&\quad + (b_1 - b_2)\zeta_3^+\zeta_4^+ + \frac{b_1 - b_2}{2\sqrt{b_2 - \lambda}}\left[{\zeta_3^+}^2\left(e^{2\sqrt{b_2-\lambda}} - e^{\sqrt{b_2-\lambda}}\right) + {\zeta_4^+}^2\left(e^{-\sqrt{b_2-\lambda}} - e^{-2\sqrt{b_2-\lambda}}\right)\right],
\end{aligned}
\tag{2.11}
$$

where ζ^+ is the same as ξ^+ in (2.4) with (a, b, κ, s) replaced by $(a_2, b_2, \kappa_2, 1/2)$, κ_2 is the same as κ in (2.3) with (a, b, s) replaced by $(a_2, b_2, 1/2)$.

Fig. 4 shows regions of the (a_1, λ) plane where the integrals I_1, I_2 are negative. The shaded region is where both I_1 and I_2 are negative, i.e. where ground state existence is guaranteed irrespectively of the coefficients Γ_1, Γ_2 and of p (within (H1)-(H3)). Similarly to Fig. 1 we covered the region $\{(a_1, \lambda) \in \mathbb{R}^2 : -1 \le a_1 \le 1.5, -1.5 \le \lambda \le \min\{a_1, a_2, b_1, b_2\} - 0.0256\}$ completely with squares of size 0.0056 in each dimension and used interval arithmetic to evaluate I_1 and I_2.

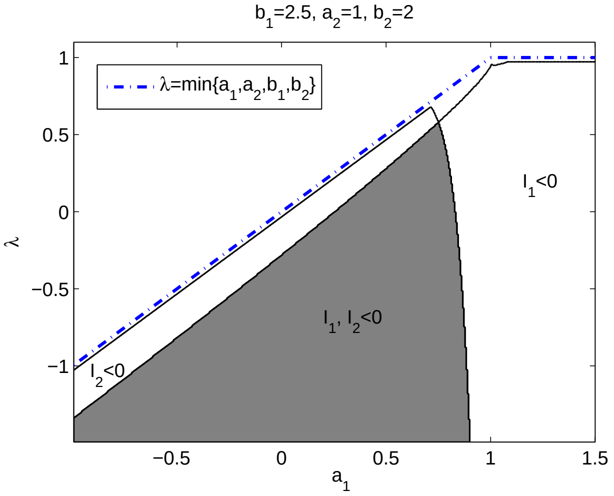

FIGURE 4. Region in the (a_1, λ) plane, where suprema of the enclosures of I_1, I_2 are negative for the interface (1.2) with piecewise constant V_1 and V_2 and $b_1 = 2.5, a_2 = 2, b_2 = 2, s_1 = s_2 = \frac{1}{2}$ (computations performed in interval arithmetic).

In Fig. 5 the enclosures of $\sqrt{a_1 - \lambda}\sqrt{b_1 - \lambda}\ I_1$ and $\sqrt{a_2 - \lambda}\sqrt{b_2 - \lambda}\ I_2$ as functions of a_1 are plotted for the example in Fig. 4 at two values of λ. At $\lambda = 0.8$ the value of I_2 is always positive while at $\lambda = 0$ both I_1 and I_2 are verified negative for $a_1 \in (0.11, 0.85)$, where ground state existence thus follows.

3. PIECEWISE LINEAR POTENTIALS V_1 AND V_2

Here we consider continuous piecewise linear functions as potentials. Unlike in the case of piecewise constant potentials in Section 2, explicit formulas for the Bloch modes $u_\pm$ are now

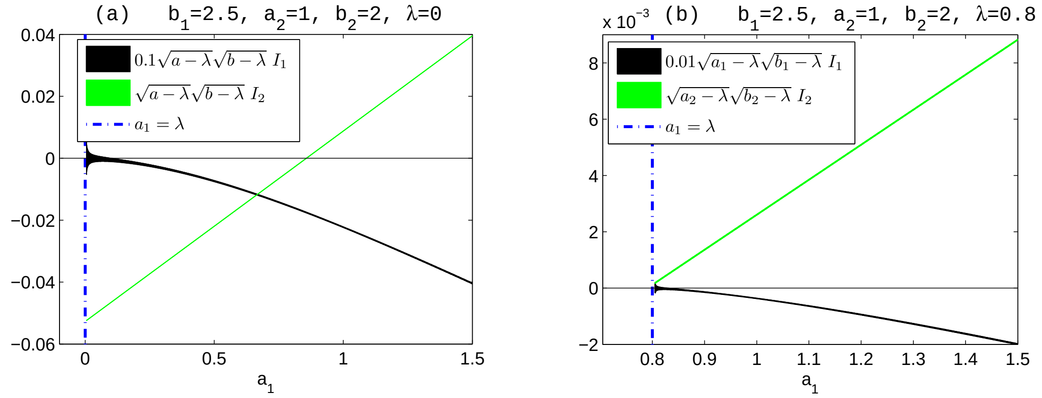

FIGURE 5. Scaled plots of the interval enclosures of $\sqrt{a_1-\lambda}\sqrt{b_1-\lambda}\ I_1$ and $\sqrt{a_2-\lambda}\sqrt{b_2-\lambda}\ I_2$ as functions of a_1 with a_2, b_1 and b_2 as in Fig. 4. In (a) $\lambda = 0$ and in (b) $\lambda = 0.8$ (computations performed in interval arithmetic with the a_1-interval width 1/1000).

generally not available. We compute the Bloch waves via the numerical enclosure method presented in [7]. All presented results are therefore verified.

Example 1. Let us consider the dislocation interface (1.6) with $\tau_1 = \tau_2 =: \tau$ for the following 1-periodic potential

$$V_0(x) = \begin{cases} 4x-1, & x \in [0.25, 0.5], \\ -4x+3, & x \in [0.5, 0.75], \\ 0, & x \in [0, 0.25] \cup [0.75, 1], \end{cases}$$

cf. Fig. 6.

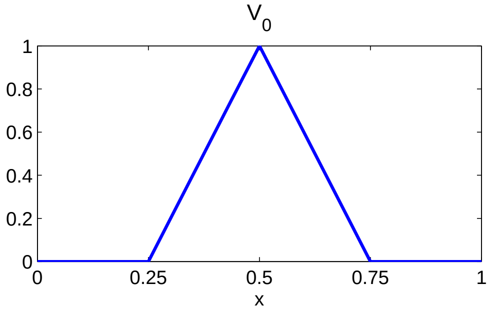

FIGURE 6. Potential $V_0(x)$ on its period for example 1

Let u_+ and u_- be the fundamental solutions of

$$-u'' + (V_0(x) - \lambda)u = 0$$

with the form

$$u_+(x) = e^{-\kappa x} p_+(x),\ u_-(x) = e^{\kappa x} p_-(x), \tag{3.1}$$

where $\kappa > 0$ is the characteristic exponent and p_+, p_- are $1-$periodic functions. Note that for $\rho := e^{\kappa} > 1$

$$u_+(x+1) = \rho^{-1} u_+(x),\ u_-(x+1) = \rho u_-(x)$$

hold.

Since $V_0(x)$ is an even function, $u_+(-x)$ is also a fundamental solution. $u_+(-x)$ must be a linear combination first of both $u_-(x)$ and $u_+(x)$, but since $u_+(x)$ grows at $-\infty$ whereas $u_+(-x)$ and $u_-(x)$ both decay at $-\infty$, the factor of $u_+(x)$ in the linear combination must be zero, i.e. $u_+(-x) = cu_-(x)$ holds for some $c \in \mathbb{C}$. Noting that the fundamental solutions can be normalized, we can define

$$u_+(x) := u_-(-x)$$

after computing $u_-(x)$. Then by simple calculations we see that $I_1 = I_2$ holds.

In Fig. 7 the enclosure of I_1 as a function of τ is plotted for the two cases: (a) $\lambda = -1$, (b) $\lambda = -0.1$. In case of (a) I_1 is negative for $\tau \in [0.04, 0.49]$ and in case of (b) I_1 is negative for $\tau \in [0.2, 0.49]$. Hence ground states exist in these cases.

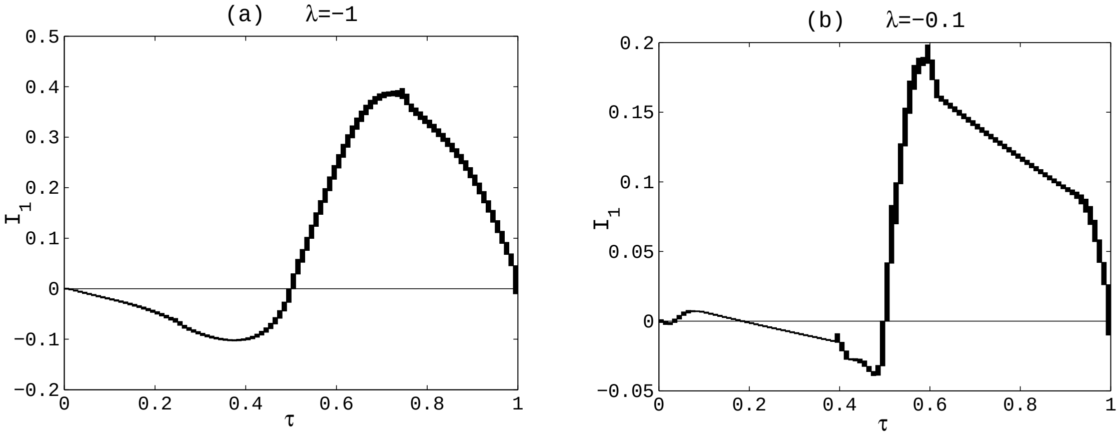

FIGURE 7. Plot of the interval enclosure of I_1 as a function of τ with interval width 0.01 for example 1.

Example 2. As another example of the dislocation interface (1.6) with $\tau_1 = \tau_2 =: \tau$ we consider the 1-periodic potential

$$V_0(x) = \begin{cases} 30x - 4.5, & x \in [0.15, 0.25], \\ -30x + 10.5, & x \in [0.25, 0.35], \\ 0, & x \in [0, 0.15] \cup [0.35, 1] \end{cases}$$

shown in Fig. 8.

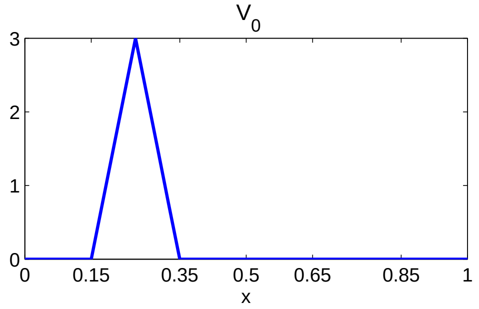

FIGURE 8. Potential $V_0(x)$ on its period for example 2

Because V_0 is not even, I_1 is generally different from I_2 and we plot in Fig. 9 the enclosure of both I_1, I_2 as functions of τ for the case (a) $\lambda = -1$ and (b) $\lambda = -0.01$. Several regions are observed, where I_1 or I_2 are negative and where by Theorem 1 ground state existence follows for the corresponding interfaces (1.6). As in Section 2 we also find intervals where both I_1 and I_2 are negative so that ground states exist for arbitrary Γ_1, Γ_2 and p (within H1-H3). In case (a) both I_1 and I_2 are negative for $\tau \in [0.01, 0.31] \cup [0.51, 0.66]$ and in case of (b) both I_1 and I_2 are negative for $\tau \in [0.18, 0.31]$.

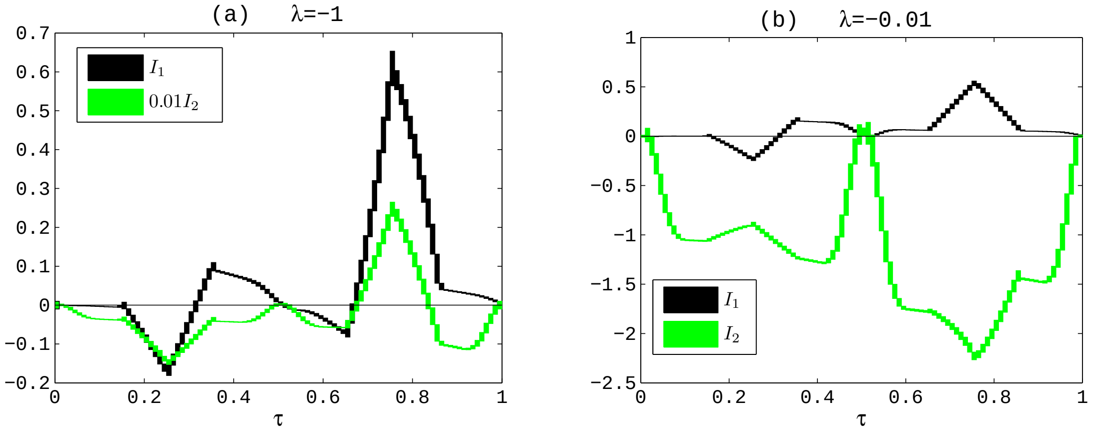

FIGURE 9. Plot of the interval enclosure of I_1, I_2 as functions of τ with interval width 0.01 for example 2.

Example 3. Here we consider a general interface (1.2) with piecewise linear V_1, V_2. As explained in Section 2.3, we need to show that *both* I_1 and I_2 are negative in order for Theorem 1 to yield ground state existence. As we noted below Corollary 2, we should violate a monotone order between V_1 and V_2 in order to possibly obtain negative I_1 and I_2 simultaneously.

An example of potentials satisfying both $I_1 < 0$ and $I_2 < 0$ is

$$V_1(x) = \begin{cases} 2000x - 400, & x \in [0.2, 0.25], \\ -2000x + 600, & x \in [0.25, 0.3], \\ 0, & x \in [0, 0.2] \cup [0.3, 1], \end{cases} \tag{3.2}$$

$$V_2(x) = \begin{cases} 20x - 14, & x \in [0.7, 0.75], \\ -20x + 16, & x \in [0.75, 0.8], \\ 0, & x \in [0, 0.7] \cup [0.8, 1], \end{cases} \tag{3.3}$$

see Fig. 10 (a).

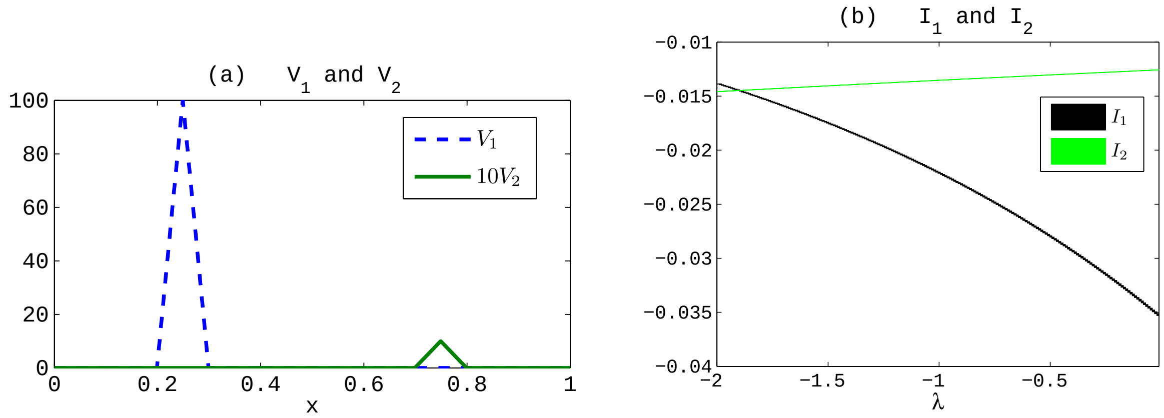

Figure 10. (a) Potentials $V_1(x)$ and $V_2(x)$ in (3.2), (3.3) on their period. (b) Interval enclosure of I_1, I_2 as functions of λ with interval width 0.01 for potentials in (3.2), (3.3).

We have verified that for $\lambda \in [-2, -0.01]$ both I_1 and I_2 are negative. We plot in Fig. 10 (b) the enclosure of both I_1, I_2 as functions of λ using intervals with width 0.01.

In case that supp(V_2) is closer to supp(V_1) as follows (see Fig. 11), we verified that I_1 is negative and I_2 is positive for $\lambda \in [-2, -0.01]$, whence ground state existence cannot be concluded using Theorem 1.

$$V_1(x) = \begin{cases} 2000x - 400, & x \in [0.2, 0.25], \\ -2000x + 600, & x \in [0.25, 0.3], \\ 0, & x \in [0, 0.2] \cup [0.3, 1]. \end{cases} \tag{3.4}$$

$$V_2(x) = \begin{cases} 20x - 6.5, & x \in [0.325, 0.375], \\ -20x + 8.5, & x \in [0.375, 0.425], \\ 0, & x \in [0, 0.325] \cup [0.425, 1]. \end{cases} \tag{3.5}$$

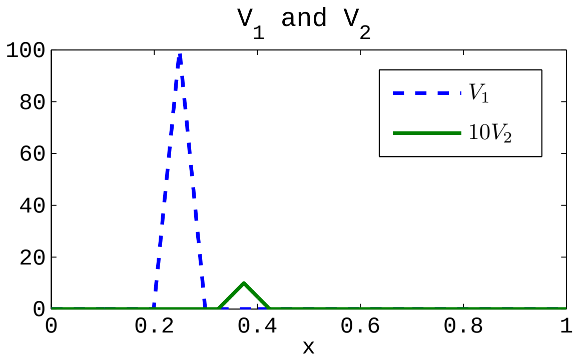

FIGURE 11. Potentials $V_1(x)$ and $V_2(x)$ in (3.4) and (3.5) on their period.

REFERENCES

[1] E. Blank and T. Dohnal. Families of Surface Gap Solitons and their Stability via the Numerical Evans Function Method. *SIAM J. Appl. Dyn. Syst.*, 10:667–706, 2011.

[2] T. Dohnal and D.E. Pelinovsky. Surface Gap Solitons at a Nonlinearity Interface. *SIAM J. Appl. Dyn. Syst.*, 7:249–264, 2008.

[3] T. Dohnal, M. Plum, and W. Reichel. Surface gap soliton ground states for the nonlinear Schrödinger equation. *Comm. Math. Phys.*, 308:511–542, 2011.

[4] M.S.P. Eastham. *Spectral Theory of Periodic Differential Equations.* Scottish Academic Press, Edinburgh London, 1973.

[5] Y. V. Kartashov, V. A. Vysloukh, and L. Torner. Surface gap solitons. *Phys. Rev. Lett.*, 96:073901, 2006.

[6] K.G. Makris, J. Hudock, D.N. Christodoulides, G.I. Stegeman, O. Manela, and M. Segev. Surface lattice solitons. *Opt. Lett.*, 31(18):2774–2776, 2006.

[7] K. Nagatou. Validated computations for fundamental solutions of linear ordinary differential equations. *International Series of Numerical Mathematics*, 157:43–50, 2008.

[8] A. Pankov. Periodic nonlinear Schrödinger equation with application to photonic crystals. *Milan J. Math.*, 73:259–287, 2005.

[9] Ch.R. Rosberg, D.N. Neshev, W. Krolikowski, A. Mitchell, R.A. Vicencio, M.I. Molina, and Y.S. Kivshar. Observation of surface gap solitons in semi-infinite waveguide arrays. *Phys. Rev. Lett.*, 97:083901, 2006.

[10] S.M. Rump. INTLAB - INTerval LABoratory. In Tibor Csendes, editor, *Developments in Reliable Computing*, pages 77–104. Kluwer Academic Publishers, Dordrecht, 1999. http://www.ti3.tu-harburg.de/rump/.

[11] S. Suntsov, K. Makris, D. Christodoulides, G. Stegeman, R. Morandotti, M. Volatier, V. Aimez, R. Arés, E. Yang, and G. Salamo. Optical spatial solitons at the interface between two dissimilar periodic media: theory and experiment. *Opt. Express*, 16:10480–10492, 2008.

[12] A. Szameit, Y. Kartashov, F. Dreisow, T. Pertsch, S. Nolte, A. Tünnermann, and L. Torner. Observation of Two-Dimensional Surface Solitons in Asymmetric Waveguide Arrays. *Phys. Rev. Lett.*, 98:173903, 2007.

T. Dohnal
Institut für Angewandte und Numerische Mathematik, Karlsruhe Institute of Technology (KIT)
D-76128 Karlsruhe, Germany
E-mail address: `dohnal@kit.edu`

K. Nagatou
Institute of Mathematics for Industry, Kyushu University
819-0395 Fukuoka, Japan
E-mail address: `nagatou@imi.kyushu-u.ac.jp`

M. Plum
Institut für Analysis, Karlsruhe Institute of Technology (KIT)
D-76128 Karlsruhe, Germany
E-mail address: `michael.plum@kit.edu`

W. Reichel
Institut für Analysis, Karlsruhe Institute of Technology (KIT)
D-76128 Karlsruhe, Germany
E-mail address: `wolfgang.reichel@kit.edu`